

See discussions, stats, and author profiles for this publication at: <https://www.researchgate.net/publication/7361458>

Probing the Acidity of *p*-Substituted Phenols in the Excited State: Electronic Spectroscopy of the *p*-Cyanophenol–Water Cluster

ARTICLE *in* CHEMPHYSCHEM · FEBRUARY 2006

Impact Factor: 3.42 · DOI: 10.1002/cphc.200500365 · Source: PubMed

CITATIONS

6

READS

107

5 AUTHORS, INCLUDING:



[Michael Schmitt](#)

Heinrich-Heine-Universität Düsseldorf

83 PUBLICATIONS 1,384 CITATIONS

SEE PROFILE

Probing the Acidity of *p*-Substituted Phenols in the Excited State: Electronic Spectroscopy of the *p*-Cyanophenol–Water Cluster

Christoph Jacoby,^[a, b] Marcel Böhm,^[a] Chau Vu,^[a] Christian Ratzer,^[a] and Michael Schmitt^{*[a]}

The hydrogen bond structure of the *p*-cyanophenol–water cluster has been determined in the ground and first excited electronic state by rotationally resolved UV spectroscopy. The water molecule is *trans*-linearly bound to the hydroxy group of the *p*-cyanophenol moiety, with hydrogen bond distances considerably shorter in both electronic states than in the similar phenol–water cluster. The structure of the cluster has been elucidated by *ab initio*

calculations at various levels of theory and compared to the experimental findings. The barriers to internal rotation of the water moiety were determined experimentally to be 275 and 183 cm^{−1} for the ground and excited state, respectively. Hydrogen bond distances and the energy barrier to water torsion correlate with the *pK_a* values of different substituted phenols for both electronic states.

1. Introduction

Hydrogen-bonded clusters of phenol and substituted phenols have found considerable interest as model systems for solvation processes, electronic ground and excited state acidities, and dynamical processes connecting the primary excited state with the electronic ground state. While the phenol–water system has been studied in great detail experimentally and theoretically for both the electronic ground and excited state, little is known about the different substituted phenol–water clusters. Substitution in the *para* position with respect to the hydroxy group allows the study of electronic effects on hydrogen bonding with minimized sterical perturbations. A very interesting system is the *p*-cyanophenol–water cluster, because the cyano group exerts a strong mesomeric effect, which drastically alters properties, like acidities, lifetimes, and excited state structures of both the monomer and the water cluster. Both functional groups in *p*-cyanophenol (*p*-CP), the hydroxy group as well as the cyano group, may bind a water molecule in the binary *p*-CP–water cluster. The geometry of the *p*-CP monomer can be derived from the structures of phenol and benzonitrile. Its water cluster might therefore be *trans*-linearly hydrogen bound via the hydroxy group as in the case of phenol–water,^[1–3] or doubly hydrogen bound via the cyano group and the *ortho* hydrogen atom of the aromatic ring.^[4,5]

The complete substitution structure of the phenol in the electronic ground state was determined by Larsen and co-workers^[6,7] with microwave spectroscopy. The electronically excited state was examined by Martinez et al.^[8] and Berden et al.^[1] with laser-induced fluorescence spectroscopy (LIF) and by Helm et al.^[9] with resonant two photon ionization (R2PI) spectroscopy. From rotationally resolved spectroscopic studies of isotopomers Ratzer et al.^[10] have proposed a partial substitution structure for the electronic excited state of phenol.

The ground state of benzonitrile has also been studied by microwave spectroscopy.^[11,12] The electronic excited state was investigated using high-resolution laser spectroscopy by Helm et al.^[13] From the long fluorescence lifetime of benzonitrile they excluded that the charge transfer (CT) state, in which the CN group is nonlinear, is located below the locally excited *S*₁ state. Borst et al.^[14] determined the dipole moment of benzonitrile in both electronic states by Stark effect studies of the electronic spectra and found the additivity rule of incremental dipole moments to be valid for the planar *S*₁ state.

Roth et al. determined the vibrational frequencies of *p*-CP in the electronic ground state through laser induced dispersed fluorescence spectra and compared them to *ab initio* normal mode vibrational frequencies.^[15] A rotationally resolved spectrum of the *S*₁ ← *S*₀ vibronic origin transition of *p*-CP was reported by Küpper et al.^[16] From the changes of the rotational constants upon electronic excitation they postulated a quinoïdal distortion of the aromatic ring.

The *pK_a* value of *p*-CP was determined to be 7.74 in the *S*₀ state and 3.33 in the *S*₁ state,^[17] thus *p*-CP is a stronger acid than phenol in both electronic states. Furthermore, the in-

[a] Dr. C. Jacoby, M. Böhm, C. Vu, Dr. C. Ratzer, Dr. M. Schmitt
Heinrich-Heine-Universität, Institut für Physikalische Chemie
40225 Düsseldorf, Germany
Fax: (+49) 211-81-15195
E-mail: mschmitt@uni-duesseldorf.de

[b] Dr. C. Jacoby
Current address:
Heinrich-Heine-Universität Düsseldorf
Institut für Herz- und Kreislaufphysiologie
40225 Düsseldorf, Germany

crease in acidity upon electronic excitation of *p*-CP is larger than that of phenol.

The binary *p*-CP-(H₂O)₁ cluster was studied by using fluorescence excitation, resonance enhanced multiphoton ionization (REMPI), hole-burning, and fluorescence detected IR spectroscopy by Biswas et al.^[18] They performed ab initio calculations on different isomers of the clusters and found the stabilization energy of the ring-like cyano bound structure to be about 18 kJ mol⁻¹ smaller than that of the *trans*-linearly hydroxy bound structure. It was proved by hole-burning spectroscopy, that only one isomer is contributing to the electronic spectrum up to 800 cm⁻¹ above the electronic origin. Leutwyler et al.^[19] reported the structures of the *p*-CP-(H₂O)₂ cluster and postulated a cyclic structure with both water moieties bound to the hydroxy group.

Herein, we investigate the influence of the altered acidity in both electronic states on the molecular properties of the *p*-CP binary water cluster.

Experimental Section

The experimental setup for the rotationally resolved LIF is described in detail elsewhere.^[20] Briefly, it consists of a ring dye laser (Coherent 899-21) operated with Rhodamine 110, pumped with 6 W from an Ar⁺-ion laser (514 nm). The light was coupled into an external folded ring cavity (Spectra Physics) for second harmonic generation (SHG). *p*-CP was purchased from Fluka (> 97%). The molecular beam was formed by coexpanding *p*-CP (at 190 °C and 5 mbar H₂O seeded in 600 mbar of argon) through a 100 μm nozzle into the vacuum. The molecular beam machine consists of three differentially pumped vacuum chambers that are linearly connected by skimmers (1 mm and 3 mm) in order to reduce the Doppler width. The molecular beam is crossed at right angles in the third chamber with the laser beam 360 mm downstream of the nozzle. The resulting fluorescence is collected perpendicular to the plane defined by the laser and the molecular beam by an imaging optics setup consisting of a concave mirror and two plano-convex lenses. The resulting Doppler width in this setup is 25 MHz (FWHM). The integrated molecular fluorescence is detected by a photomultiplier tube, whose output is discriminated and digitized by a photon counter and transmitted to a PC for data recording and processing.

The ab initio calculations have been performed using Gaussian 98.^[21] The SCF (self-consistent-field) convergence criterion used for our calculations was an energy change below 10⁻⁸ Hartree, while the convergence criterion for the gradient optimization of the molecular geometry was $\partial E/\partial r < 1.5 \times 10^{-5}$ Hartree/Bohr and $\partial E/\partial \phi < 1.5 \times 10^{-5}$ Hartree/degrees. A normal mode analysis was performed utilizing the analytical second derivatives of the potential energy surface. The basis set superposition error (BSSE), of the binding energy of the cluster, was corrected for using the counterpoise method from Boys and Bernardi.^[22] The electronically excited state has been optimized with complete active space, (CAS), SCF using an active space of 12 electrons in 11 orbitals. Additionally, the geometry of the electronically excited state has been optimized using time-dependent density functional theory (TDDFT)^[23,24] employing the B3-LYP functional.^[25,26] These calculations were performed with the program system TURBOMOLE.^[27,28]

2. Results and Discussion

Figure 1 presents the rotationally resolved electronic spectrum of the origin of the binary *p*-CP–water cluster at 35304.46 cm⁻¹. This origin band is red shifted by 243 cm⁻¹ relative to the origin of the *p*-CP monomer. The spectrum of the electronic origin is split into two subbands due to the internal

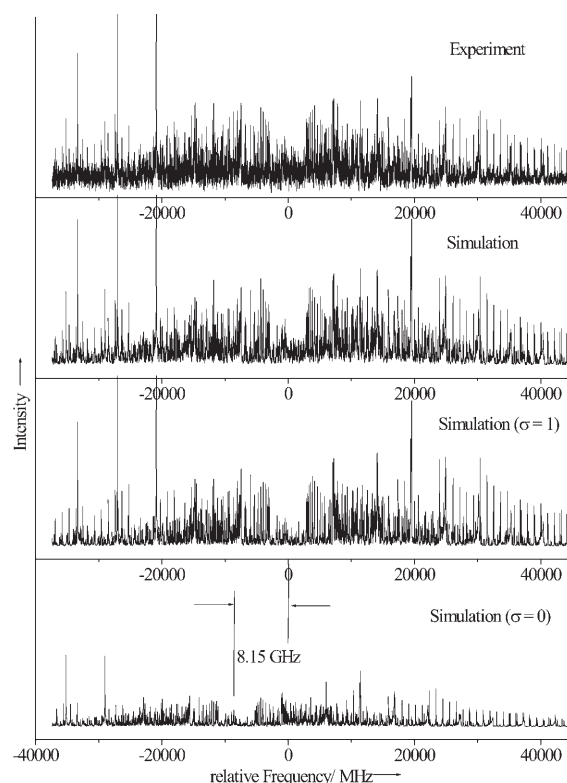


Figure 1. Rotationally resolved electronic spectrum of the origin of the *p*-cyanophenol–water cluster. From top to bottom: experimental spectrum, simulated spectrum using the parameters from Table 1, separate simulations of the torsional subbands.

rotation of the water moiety. The molecular symmetry group, which takes this motion into account, is G_4 , isomorphic with the point group C_{2v} . The lowest torsional state (with $\sigma=0$) is of *A* symmetry, the following energetical state (with $\sigma=1$) is of *B* symmetry. Both subbands can be fitted using rigid asymmetric rotor selection rules with two sets of rotational constants and with the difference of the vibronic origins as an additional parameter. The theory of coupling of the two-fold internal rotation of the water moiety to the overall rotation of the cluster has been elaborated in detail in refs. [1] and [29] and will not be repeated here. The upper trace of Figure 1 shows the experimental spectrum, the following trace the complete simulation using the parameters from Table 1. The next two traces give the individual simulations for the two torsional subbands caused by the internal rotation of the water moiety. A zoomed in portion of the spectrum is shown in Figure 2.

The spectrum was automatically assigned using the genetic algorithm (GA) based fitting procedure described in refs. [30] and [31]. Since the GA performs a fit of the shape of the com-

Table 1. Molecular parameters of *p*-cyanophenol–water from the GA fit. The doubly primed parameters refer to the electronic ground state. ΔA , ΔB , and ΔC are defined as $A'-A''$, etc. with the singly primed rotational constants describing the electronically excited state. The numbers in parentheses give the standard deviations of the parameters to the number of quoted digits.

<i>p</i> -CP(H ₂ O) ₁	$\sigma=0$	$\sigma=1$
A'' [MHz]	3462.16(50)	3459.95(6)
B'' [MHz]	587.87(8)	588.00(4)
C'' [MHz]	503.62(6)	503.75(2)
ΔA [MHz]	−48.69(24)	−50.39(5)
ΔB [MHz]	−0.11(1)	−0.13(1)
ΔC [MHz]	−1.08(1)	−1.06(1)
θ [°]	69.5(13)	74.48(45)
$\Delta\nu(\text{Lorentz})$ [MHz]		15.7(10)
τ [ns]		10.1(5)
ν_0 [cm ^{−1}]	35304.46(2)	35304.70(2)
$\nu_0(A) - \nu_0(B)$ [MHz]		−8149.42(106)

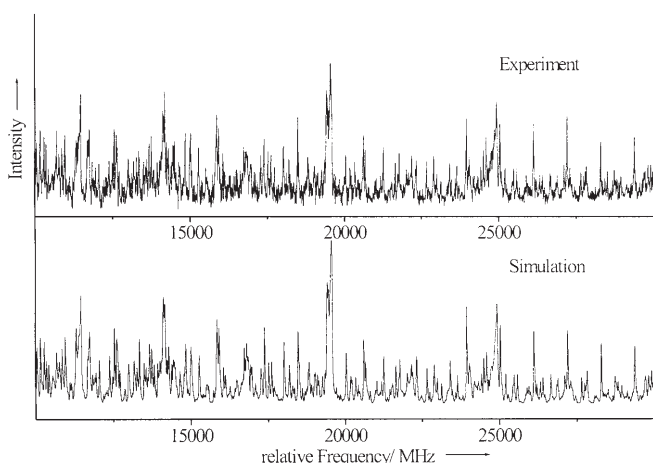


Figure 2. Magnified 20 GHz portion in the R-branch of the origin of *p*-cyanophenol–water. Upper trace: experimental spectrum, lower trace: simulated spectrum.

plete spectrum, more accurate results on the lineshape parameters are obtained than from a lineshape fitted to a few selected individual lines. The following parameters were used in the GA fit:

- (i) the rotational constants A , B , and C of both torsional components for the electronic ground and excited state
- (ii) the center frequency ν_0 of the first torsional band
- (iii) the difference of the center frequencies of the torsional subbands
- (iv) the angle θ of the transition dipole moment with the inertial a -axis
- (v) the Lorentzian contribution $\Delta\nu(\text{Lorentz})$ to the Voigt profile with a fixed Doppler width of 25 MHz. Even for Lorentz contributions well below the Doppler width quite accurate values are obtained because all the lines in the experimental spectrum are included in the lineshape fit.
- (vi) two temperatures and a weight factor given by Equation (1):

$$n(T_1, T_2, w) = e^{-\frac{E}{kT_1}} + we^{-\frac{E}{kT_2}} \quad (1)$$

where E is the energy of the lower state, k is the Boltzmann constant, w is a weighting factor, and T_1 and T_2 are the temperatures.^[32] The resulting temperatures and weights obtained from the individual spectra are not presented in Table 1 as they are strongly correlated and are merely used to facilitate the intensity fit for low and high J states simultaneously.

The resulting molecular parameters are given in Table 1. The spectrum is an *ab*-hybrid band with 93% *b*-type and 7% *a*-type character and is split into two subbands by the internal rotation of the water moiety, with the low frequency component having 1/3 of the intensity of the high-frequency component. The splitting between the origins of the two subbands amounts to 8149 MHz (0.27 cm^{−1}). The total spectrum contains about 7500 rovibronic lines with a Lorentzian linewidth of 15.7(10) MHz, leading to an excited state lifetime of 10.1(5) ns. (The numbers in parentheses give the standard deviations of the parameters to the number of quoted digits.) This lifetime is within the same accuracy as that of the *p*-CP monomer (10.6 ns).

2.1. Determination of the Intermolecular Structure

The program pKFit^[10] was used to determine the intermolecular structure of *p*-CP–water in the S_0 and S_1 states from the rotational constants given in Table 1. Due to the very limited number of inertial parameters, we performed a fit limited to the partial r_0 structure, which neglects all vibrational contributions.

The change of the *p*-CP monomer geometry upon electronic excitation has been taken from ref. [16]. The mean aromatic C–C bond length in the ground state was determined to be 139.4 pm, increasing to 143.9 upon excitation. Keeping the geometries from ref. [16] fixed together with a fixed water geometry ($R_{\text{OH}} = 0.957$ Å, $\text{H-O-H} = 104.52^\circ$ from ref. [33]) we fitted the O_7O_{15} distance, the $\text{O}_7\text{H}_8\text{O}_{15}$ angle, and the $\text{H}_8\text{O}_{15}\text{H}_{17}$ angle (cf. Figure 3 for the atomic numbering). The other three intermolecular parameters are kept fixed to the values of a planar *trans*-linear cluster: dihedral ($\text{C}_1\text{O}_7\text{H}_8\text{O}_{15}$) = 180° and dihedral ($\text{O}_7\text{H}_8\text{O}_{15}\text{H}_{16}$) = $-\text{dihedral}(\text{O}_7\text{H}_8\text{O}_{15}\text{H}_{17}) = 60^\circ$. The last two parameters are restricted under the assumption that one of the water lone pairs points towards the hydroxy group. They have opposing signs due to symmetry restrictions. Using this model, we obtained a hydrogen bond length of 282.8(1) pm in the S_0 state and of 269.0(1) pm in the S_1 state. Both values are considerably shorter than the corresponding distances in the phenol–water (293 and 289 pm, respectively). The $\text{O}_7\text{H}_8\text{O}_{15}$ angle was determined to be $177.2(3)^\circ$ in the S_0 state and $179.0(4)^\circ$ in the

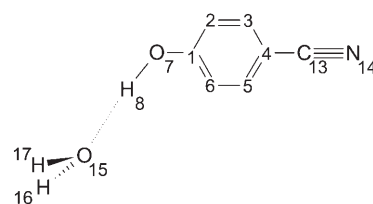


Figure 3. Atomic numbering used in the geometry fit of *p*-CP–water.

S_1 state, and the $H_8O_{15}H_{17}$ angle was determined to be $115(2)^\circ(S_0)$ and $111(4)^\circ(S_1)$. The geometry parameters are summarized in Table 2 and compared to the results of ab initio calculations. The change of the hydrogen bond length upon electronic excitation is larger than in the structurally similar phenol–water cluster. These changes reflect both the higher ground state acidity of *p*-CP ($pK_a=7.74$) compared to phenol ($pK_a=9.86$), and the larger increase of acidity in *p*-CP upon electronic excitation [$pK_a(\text{phenol}, S_1)=6$ vs $pK_a(p\text{-CP}, S_1)=3.33$].

Table 2. Intermolecular geometry parameters of the *p*-CP–water cluster. The distance (R) is given in pm, angles (A) and dihedral angles (D) in degrees.

	Exp. (S_0)	Exp. (S_1)	MP2 (S_0)	HF (S_0)	CIS (S_1)	DFT (S_0)	TDDFT (S_1)
$R(O_7O_{15})$	282.8	269.0	280.49	287.19	284.90	276.79	270.26
$A(O_7H_8O_{15})$	177.2	178.9	178.734	177.883	178.870	179.628	176.265
$A(H_8O_{15}H_{17})$	115.0	111.4	113.362	118.841	120.033	113.976	113.204
$D(C_1O_7H_8O_{15})$	180 ^[a]	180 ^[a]	179.622	179.992	179.858	178.770	179.887
$D(O_7H_8O_{15}H_{16})$	−60 ^[a]	−60 ^[a]	−59.474	−66.533	−68.106	−61.013	−59.044
$D(O_7H_8O_{15}H_{17})$	60 ^[a]	60 ^[a]	60.230	66.551	68.374	58.681	58.879

[a] Kept fixed at this value.

2.2. Barriers to Internal Rotation of the Water Moiety

The barriers to rotation of the water moiety have been estimated using the program HTorFit. The underlying theory for treating the twofold internal rotation in the frame of the principal axis method (PAM)^[34] is given in ref. [29].

Three pieces of information, which can be used for the determination of the torsional barriers, can be extracted from the rovibronic spectrum: (i) the subtorsional splitting arising from transitions belonging to the different torsional components of σ with the selection rule $\Delta\sigma=0$, (ii) the difference in the rotational constants of the two different components of σ in the ground state, and (iii) this difference in the electronically excited state. The subtorsional splitting between the transitions $(\sigma=0)' \leftarrow (\sigma=0)''$ and $(\sigma=1)' \leftarrow (\sigma=1)''$ was determined to be 8149.42(106) MHz. This splitting, together with the differences in the rotational constants of the $(\sigma=0)$ and $(\sigma=1)$ levels in the electronic ground and excited state, which contain the second-order perturbation coefficients, have been used to fit the barrier to the water torsional motion. Unfortunately, for *p*-CP–water no additional torsional data are available as for the similar phenol–water cluster.^[29,35] Thus, we were not able to independently fit the barriers and the torsional constants for both electronic states.

The barriers, which are obtained from this analysis, are effective barriers because the actual motion is more complex than a simple one-dimensional torsion.^[2,3] The potential energy in this one-dimensional model is given in Equation (2). It depends only on the torsional coordinate, which is defined by rotation about the symmetry axis of the water molecule:

$$V(\tau) = \frac{1}{2} V_2 (1 - \cos 2\alpha). \quad (2)$$

Figure 4 shows why the path, which connects the identical minima that arise from permutation of H1 and H2, cannot be the simple torsion about the water symmetry axis. This motion would break the hydrogen bond between the localized molecular orbital (MO) (1) of the water moiety and the phenolic hydroxy group. The new hydrogen bond would then be formed using the MO (2). The (1,2) permutation of the hydrogen atom can also be achieved in a “smoother” pathway. Rotation about the hydrogen bond would convert the cluster into the *cis* conformer.

To bring it back to the most stable *trans* configuration, an inversion^[3] or wagging motion^[2] would then change the MO involved in the hydrogen bonding. The effective barrier arises from a concerted (coupled) motion along both coordinates, constituting the minimum energy path.

With the one-dimensional model we fit the effective barriers using the value for the tor-

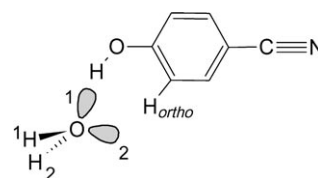


Figure 4. Schematic representation of the localized molecular orbitals of the water moiety involved in the hydrogen bonding of the cluster. The indices 1 and 2 are used for numbering the atoms to describe the permutation (1,2). For numbering of lone pairs see text.

sional constant F of 14.813 cm^{-1} for the electronic ground state and of 13.415 cm^{-1} for the electronically excited state. These torsional constants have been determined from the analysis of several torsional bands in different isotopomers in the phenol–water cluster.^[29] Values of $V_2''=275(4) \text{ cm}^{-1}$ and $V_2'=183(1) \text{ cm}^{-1}$ for the ground and excited state of the *p*-CP–water cluster, respectively, have been obtained. These barriers are considerably larger than the corresponding values in phenol ($V_2''=175.4 \text{ cm}^{-1}$, $V_2'=109.1 \text{ cm}^{-1}$). The reason for the strong increase of the barrier height in the electronic ground state is the formation of an additional hydrogen bond between the *ortho*-CH group in *p*-CP and phenol and the O atom of the water moiety. Feller calculated an $OH\cdots O$ distance of 185.8 pm.^[36] for the hydrogen bond in the *trans*-linear phenol–water cluster calculated at the MP2/6-31G(d,p) level. The $CH\cdots O$ distance of the *ortho*-CH group in phenol was calculated to be 270.2 pm. The $OH\cdots O$ distance in *p*-CP is decreased to 182.8 pm, and the $CH\cdots O$ distance to 263.6 pm. Both distances are smaller in *p*-CP compared to phenol due to the higher acidity of *p*-CP. The hydrogen bonds are oriented in the direction of the equivalent oxygen lone pairs of the water moiety and hinder the torsional motion. This effect is larger in *p*-CP ex-

plaining the higher barrier in the ground state. The increase of acidity upon electronic excitation is larger in *p*-CP than in phenol. Thus, also the increase in the barrier height is expected to be larger in *p*-CP as has been found experimentally.

2.3. Comparison to ab initio Calculations

The electronic ground state of the *p*-CP–water cluster has been optimized on the MP2/6-31G(d,p) level of theory. The rotational constants of the optimized structure are given in Table 3 and are compared to the results of the experiment.

Table 3. Experimental and ab initio inertial constants of the <i>p</i> -CP–water cluster. TDDFT and DFT calculations were performed with the B3-LYP functional implemented in the TURBOMOLE program system. All calculations have been performed using the 6-31G(d,p) basis set. The rotational constants are given in MHz.							
	Exp.	MP2	HF	CIS	CIS-HF	DFT/TDDFT	CAS(12/11)
<i>A</i> ''	3461.06	3413	3481	-	-	3422 ^[a]	3439 ^[a]
<i>B</i> ''	587.93	586	591	-	-	601 ^[a]	582 ^[a]
<i>C</i> ''	503.70	501	506	-	-	512 ^[a]	499 ^[a]
<i>A</i> '	3411.56	-	-	3410	-	3390 ^[b]	3332 ^[b]
<i>B</i> '	587.81	-	-	591	-	599 ^[b]	576 ^[b]
<i>C</i> '	502.63	-	-	505	-	510 ^[b]	492 ^[b]
ΔA	-49.50	-	-	-	-71	-32	-107
ΔB	-0.12	-	-	-	0	-2	-6
ΔC	-1.07	-	-	-	1	-2	7

[a] Geometry optimized to the *S*₀ state. [b] Geometry optimized to the *S*₁ state.

The deviations are less than 2% for each of the rotational constants. The MP2 stabilization energy of the cluster, including zero-point energy and BSSE corrections, amounts to 27.43 kJ mol⁻¹ (2293.04 cm⁻¹), considerably stronger than the calculated binding energy of 22.93 kJ mol⁻¹ for phenol–water using the same method and basis set. Without any symmetry constraints in the calculations, the O₇O₁₅ hydrogen bond distance (cf. Figure 3 for atomic numbering) was found to be 280.49 pm on MP2 level. The water oxygen atom is positioned in the aromatic plane [dihedral angle (C₁O₇H₈O₁₅) = 179.622°]. The hydrogen bond is linear [angle (O₇H₈O₁₅) = 178.734°] and the water molecule is oriented symmetrically about the aromatic plane [dihedral angle (O₇H₈O₁₅H₁₆) = -dihedral angle (O₇H₈O₁₅H₁₇)], and in an *anti* position with respect to the aromatic ring [angle (H₈O₁₅H₁₇) = 113.362°].

The electronically excited state has been optimized using configuration interaction with single excitations [CIS/6-31G(d,p)]. Due to a favorable cancellation of errors, even the absolute values of the rotational constants nearly match the experimental ones for the CIS calculations. The focus of these calculations is only on the difference of the rotational constants between the CIS and HF values to compute the geometry changes upon electronic excitation. These differences match very closely to the experimental changes of the rotational constants, which is due to the fact of equal approximations in both methods. These differences should merely be viewed as a guidance in the preliminary determination of the parameter limits for the GA fit of the spectrum. More reliable structures

for both electronic states and for the geometry changes can be obtained using density functional theory (DFT) for the ground state and TDDFT for the excited state. Table 3 shows, that using the B3-LYP functional even the absolute values match the experimentally determined rotational constants closely.

Furthermore, the electronic ground and excited states have been optimized with the complete active space SCF method [CASSCF/6-31G(d,p)] with 12 electrons in 11 orbitals. The active space employed in these calculations consists of three orbitals of π symmetry, centered in the aromatic ring: one occupied π

orbital is located at the cyano group, one at the hydroxy group, and one at the oxygen atom of the water moiety. The unoccupied orbitals comprise of three benzene-like π^* orbitals, one antibonding orbital at the cyano group, and one at the water moiety. Under these conditions, only poor agreement with the experimentally determined rotational constants is found.

Inspection of the ab initio geometry parameters in Table 3 shows that the close agreements of the absolute values for the rotational constants of Har-

tree–Fock (HF) and CIS for ground and excited state with the experimentally determined ones are due to an accidental cancellation of errors. Both HF and CIS O₇O₁₅ hydrogen bond lengths are largely overestimated, while the aromatic C–C bonds are underestimated. Also, the decrease of the O–O bond length in the *S*₁ state is largely underestimated. The comparison of the TDDFT(B3-LYP) calculations with the results of the experiment reveal a very close agreement not only for the rotational constants given in Table 3 but also for the geometry parameters summarized in Table 2.

3. Conclusions

The rotational constants obtained from the rotationally resolved LIF spectrum of the binary *p*-CP–water cluster allowed us to determine the intermolecular geometry parameters. Comparison with the results of ab initio calculations at various levels of theory showed a close agreement for the electronic ground state with the correlated MP2 results. The electronically excited state geometry can be well described using TDDFT with the B3-LYP functional and a moderate size basis set. In contrast, with CASSCF the intermolecular geometry cannot be described appropriately due to a lack of electron correlation and the limited active space employed. Anyhow, an active space of 12 electrons in 11 orbitals [CAS(12/11)] is close to the limit that can be currently calculated. Jansen and Gerhards,^[37] have shown a satisfying description of the excited phenol–water geometry which requires the addition of six electrons in

six σ -type orbitals to account for the $\sigma\pi$ and the $\sigma\sigma$ correlations. In the case of *p*-CP–water this would mean a mixed $\sigma\pi$ active space of CAS(18/17), obviously too large for a geometry optimization. Thus, we conclude, that a proper description of excited-state geometries should rely on the TDDFT calculations to describe all the relevant interactions and not on the CASSCF calculations with a too small active space.

Within the uncertainty, the excited state lifetime of the *p*-CP–water cluster is the same as the monomer lifetime. This is very different from the phenol/phenol-water case, where the lifetime increases from 2 to 15 ns upon cluster formation. Sobolewski and Domcke explained the short lifetime of phenol by tunneling through a barrier which separates the $^1\pi\sigma^*$ from the $^1\pi\pi^*$ surface and a subsequent internal conversion to the ground state through a conical intersection with the ground state.^[38] Two reasons might be possible for the longer lifetime of *p*-CP: The conical intersection with the ground state might be removed (like in the phenol-water cluster) or the barrier separating the excited states is considerably higher than in phenol. Further calculations are needed to distinguish between the two models.

Furthermore, the barriers to internal rotation of the water moiety about its symmetry axis in both electronic states were estimated. Both barrier heights and hydrogen bond lengths correlate well with the increased acidity of *p*-CP compared to phenol in both electronic states. While in the similar *p*-methylphenol-water cluster the hydrogen bond length is close to the values in phenol-water (290 pm in the S_0 state and 285 pm in the S_1 state of *p*-methylphenol-water vs. 293 and 289 pm, respectively, for phenol-water), considerably smaller values of 283 and 269 pm are found in the ground and excited state of *p*-CP–water.

Out of the three phenols compared in Table 4, *p*-methylphenol is the weakest acid in the electronic ground state and has the largest hydrogen bond distance. The O_7O_{15} hydrogen bond distances of the three *p*-substituted phenols scale nearly linearly with the pK_a -values in both electronic states as shown in Table 4 and in Figure 5.

The internal rotation of the water moiety is hindered by two intermolecular interactions: the $OH\cdots O$ hydrogen bond and the (weaker) $CH\cdots O$ hydrogen bond. The lone pairs of the oxygen atom of the water moiety point along both hydrogen bonds. Therefore, the barrier height is a function of the acidity of the hydroxy group as well as of the *ortho*-CH group, and the correlation between the pK_a values and the barrier heights is not so pronounced as in the case of the hydrogen bond length. Nev-

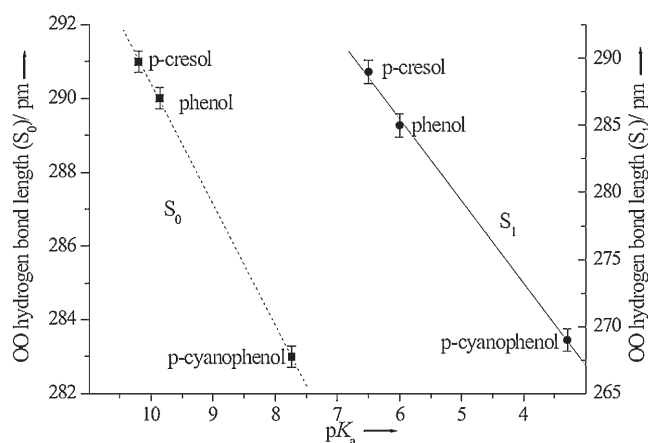


Figure 5. Correlation of the pK_a values of the monomers with the hydrogen bond length O_7O_{15} of the clusters in the electronic ground S_0 (left hand side) and excited S_1 , (right hand side) states.

ertheless, it can be inferred from Table 4, that the barrier increases with decreasing pK_a values and with decreasing (calculated) $CH\cdots O$ distances.

Acknowledgments

This work was supported by the Deutsche Forschungsgemeinschaft SCHM1043/9-4.

Keywords: acidity • cluster compounds • excited state • high-resolution UV spectroscopy • structure elucidation

- [1] G. Berden, W. L. Meerts, M. Schmitt, K. Kleinermanns, *J. Chem. Phys.* **1996**, *104*, 972–982.
- [2] M. Schütz, T. Bürgi, S. Leutwyler, T. Fischer, *J. Chem. Phys.* **1993**, *98*, 3763–3776.
- [3] S. Melandri, A. Maris, P. G. Favero, W. Caminati, *Chem. Phys.* **2002**, *283*, 185–192.
- [4] R. M. Helm, H. P. Vogel, H. J. Neusser, V. Storm, D. Consalvo, H. Dreizler, *Z. Naturforsch. A* **1997**, *52*, 655–664.
- [5] S. Melandri, D. Consalvo, W. Caminati, P. G. Favero, *J. Chem. Phys.* **1999**, *111*, 3874–3879.
- [6] T. Pedersen, N. W. Larsen, L. Nygaard, *J. Mol. Struct.* **1969**, *4*, 59–77.
- [7] N. W. Larsen, *J. Mol. Struct.* **1979**, *51*, 175–190.
- [8] S. J. Martinez, J. C. Alfano, D. H. Levy, *J. Mol. Spectrosc.* **1992**, *152*, 80–88.
- [9] R. M. Helm, H. P. Vogel, H. J. Neusser, *J. Chem. Phys.* **1998**, *108*, 4496–4504.

Table 4. pK_a values, hydrogen bond lengths O_7O_{15} (in pm), hydrogen bond lengths $C_6H\cdots O$ (in pm), and V_2 barriers (in cm^{-1}) to water internal rotation of phenol,^[1] *p*-methylphenol,^[39] and *p*-cyanophenol for both electronic states. The twofold barrier V_2 is defined in Equation (2).

	$pK_a(S_0)$	$O_7O_{15}(S_0)$	$V_2(S_0)$	$C_6H\cdots O^{[a]}$	$pK_a(S_1)$	$O_7O_{15}(S_1)$	$V_2(S_1)$
<i>p</i> -methylphenol	10.2	291	149	272	6.5 ^[b]	289	94
phenol	9.86	290	175	270	6	285	109
<i>p</i> -cyanophenol	7.74	283	275	264	3.33	269	183

[a] Calculated MP2 value. [b] Based on the assumption that the similar red shift of the phenol-water and the cresol-water cluster imply similar changes of acidity upon excitation.^[18]

- [10] C. Ratzner, J. Küpper, D. Spangenberg, M. Schmitt, *Chem. Phys.* **2002**, *283*, 153–169.
- [11] U. Dahmen, W. Stahl, H. Dreizler, *Ber. Bunsen-Ges.* **1994**, *98*, 970–974.
- [12] J. Casado, L. Nygaard, G. O. Sørensen, *J. Mol. Struct.* **1971**, *8*, 211–224.
- [13] R. M. Helm, H.-P. Vogel, H. J. Neusser, *Chem. Phys. Lett.* **1997**, *270*, 285–291.
- [14] D. R. Borst, T. M. Korter, D. W. Pratt, *Chem. Phys. Lett.* **2001**, *350*, 485–490.
- [15] W. Roth, P. Imhof, K. Kleinermanns, *Phys. Chem. Chem. Phys.* **2001**, *3*, 1806–1812.
- [16] J. Küpper, M. Schmitt, K. Kleinermanns, *Phys. Chem. Chem. Phys.* **2002**, *4*, 4634–4639.
- [17] S. Schulman, W. Vincent, W. Underberg, *J. Phys. Chem.* **1981**, *85*, 4068–4071.
- [18] N. Biswas, S. Wategaonkar, T. Watanabe, T. Ebata, N. Mikami, *Chem. Phys. Lett.* **2004**, *394*, 61–67.
- [19] S. Leutwyler, T. Bürgi, M. Schütz, A. Taylor, *Faraday Discuss.* **1994**, *97*, 285–297.
- [20] M. Schmitt, J. Küpper, D. Spangenberg, A. Westphal, *Chem. Phys.* **2000**, *254*, 349–361.
- [21] Gaussian 98 (Revision A.7), M. J. Frisch, G. W. Trucks, H. B. Schlegel, G. E. Scuseria, M. A. Robb, J. R. Cheeseman, V. G. Zakrzewski, J. A. Montgomery, R. E. Stratmann, J. C. Burant, S. Dapprich, J. M. Millam, A. D. Daniels, K. N. Kudin, M. C. Strain, O. Farkas, J. Tomasi, V. Barone, M. Cossi, R. Cammi, B. Mennucci, C. Pomelli, C. Adamo, S. Clifford, J. Ochterski, G. A. Petersson, P. Y. Ayala, Q. Cui, K. Morokuma, D. K. Malick, A. D. Rabuck, K. Raghavachari, J. B. Foresman, J. Cioslowski, J. V. Ortiz, B. B. Stefanov, G. Liu, A. Liashenko, P. Piskorz, I. Komaromi, R. Gomperts, R. L. Martin, D. J. Fox, T. Keith, M. A. Al-Laham, C. Y. Peng, A. Nanayakkara, C. Gonzalez, M. Challacombe, P. M. W. Gill, B. G. Johnson, W. Chen, M. W. Wong, J. L. Andres, M. Head-Gordon, E. S. Replogle, J. A. Pople, Gaussian, Inc., Pittsburgh, PA, **1998**.
- [22] S. F. Boys, F. Bernardi, *Mol. Phys.* **1970**, *19*, 553–566.
- [23] R. Bauernschmitt, R. Ahlrichs, *Chem. Phys. Lett.* **1996**, *256*, 454–464.
- [24] R. Bauernschmitt, M. Häser, O. Treutler, R. Ahlrichs, *Chem. Phys. Lett.* **1997**, *264*, 573–578.
- [25] C. Lee, W. Yang, R. Parr, *Phys. Rev. B* **1988**, *37*, 785–789.
- [26] A. D. Becke, *J. Chem. Phys.* **1993**, *98*, 5648–5652.
- [27] R. Ahlrichs, M. Bär, H.-P. Baron, "TURBOMOLE (version 5.6)", Universität Karlsruhe, Germany, **2002**.
- [28] R. Ahlrichs, M. Bär, M. Häser, H. Horn, C. Kölmel, *Chem. Phys. Lett.* **1989**, *162*, 165–169.
- [29] C. Jacoby, M. Schmitt, *ChemPhysChem* **2004**, *5*, 1686–1694.
- [30] J. A. Hageman, R. Wehrens, R. de Gelder, W. L. Meerts, L. M. C. Buydens, *J. Chem. Phys.* **2000**, *113*, 7955–7962.
- [31] W. L. Meerts, M. Schmitt, G. Groenenboom, *Can. J. Chem.* **2004**, *82*, 804–819.
- [32] Y. R. Wu, D. H. Levy, *J. Chem. Phys.* **1989**, *91*, 5278–5284.
- [33] W. S. Benedict, N. Gailar, E. K. Plyler, *J. Chem. Phys.* **1956**, *24*, 1139–1165.
- [34] W. Gordy, R. L. Cook, *Microwave Molecular Spectra*, 3rd ed., Wiley, New York, **1984**.
- [35] M. Schmitt, C. Jacoby, K. Kleinermanns, *J. Chem. Phys.* **1998**, *108*, 4486–4495.
- [36] D. Feller, M. W. Feyereisen, *J. Comput. Chem.* **1993**, *14*, 1027–1035.
- [37] A. Jansen, M. Gerhards, *J. Chem. Phys.* **2001**, *115*, 5445–5453.
- [38] A. L. Sobolewski, W. Domcke, *J. Phys. Chem. A* **2001**, *105*, 9275–9283.
- [39] G. Myszkiewicz, W. L. Meerts, C. Ratzner, M. Schmitt, *J. Chem. Phys.* **2005**, *123*, 44304-1–44304-7.

Received: July 8, 2005

Revised: September 9, 2005

Published online on January 13, 2006